Journal of Nuclear Materials 390–391 (2009) 955–958

Contents lists available at ScienceDirect

Journal of Nuclear Materials

journal homepage: www.elsevier.com/locate/jnucmat

Study of heat flux deposition on the limiter of the Tore Supra tokamak

S. Carpentier [a,*], Y. Corre [a], M. Chantant [a], R. Daviot [a], G. Dunand [a], J.-L. Gardarein [a], J. Gunn [a], M. Kocan [a], C. Le Niliot [b], R. Mitteau [a], V. Moncada [a], P. Monier-Garbet [a], B. Pegourié [a], C. Pocheau [a], R. Reichle [a], F. Rigollet [b], F. Saint-Laurent [a], J.-M. Travère [a], E. Tsitrone [a]

[a] Ass. Euratom-CEA, DSM/IRFM, CEA Cadarache, F-13108 Saint-Paul-Lez-Durance, France
[b] Ecole Polytechnique Universitaire de Marseille, I.U.S.T.I, UMR CNRS No 6595, Technopôle de Château Gombert, F-13453 Marseille, France

ARTICLE INFO

PACS:
28.52.Fa
44.05.+e
52.30.−q
52.55.Fa

ABSTRACT

On the limiter of Tore Supra, the heat loads map computed from deconvolution of IR surface temperatures shows good agreement with calorimetry measurements. This experimental heat pattern allows deducing the heat fluxes in the scrape-off layer using a 3D magnetic calculation and assuming only parallel heat transport along field lines. This calculation leads to an underestimation of the power circulating in the edge plasma according to the power balance, similarly to RFA measurements. The comparison between experimental heat loads on the limiter and modelling also shows a spreading of heat fluxes near the LCFS that cannot be explained only by parallel transport in the SOL.

1. Introduction

The comprehension of mechanisms governing heat flux deposition in tokamaks is an essential issue for steady state operation. The machine security and the optimisation of the plasma scenario require first, to compute heat fluxes on the plasma facing components (PFC) and, second, to understand the plasma processes that leads to these heat loads.

During operations on Tore Supra, the toroidal pumped limiter extracts more than 50% of the incident power from the plasma. The component, actively cooled and covered by CFC tiles, is designed to support a surface temperature of 1000 °C and local heat fluxes of 10 MW/m^2. A 20° section of the component is supervised by a thermography system that provides IR images with a spatial resolution of about 4 mm.

On Tore Supra, the toroidal field ripple induces a particular footprint on the component, considered as toroidally repetitive with a 20° period. Overall, this pattern shows transitions between wetted areas with long connections length (several tens of meters) and shadowed areas with very short connection lengths (several centimetres), therefore not in direct interaction with particles coming from the plasma. The wetted areas are mainly subject to high heat fluxes and erosion rate while the shadowed areas are usually subject to low heat fluxes and carbon redeposition.

In this paper we calculate the incident heat loads on the limiter and deduce from these values an estimation of the parallel heat fluxes circulating in the scrape-off layer (SOL). The experiment studied corresponds to a long duration Deuterium Inventory discharge (DITS, 2 MW of lower hybrid power injected during 125 s [1]). The experimental heat fluxes are computed on the limiter using IR images (where carbon redeposition areas are first excluded), and compared with calorimetry measurements. The heat flux map calculated in the erosion area are then transposed into the SOL and compared to the heat flux profile measured by RFA probe at the top of the machine. The agreement between the experimental heat flux map on the limiter and theoretical patterns predicted by edge plasma models is also discussed.

2. Calculation of the incident heat fluxes on the limiter

2.1. Localisation of carbon surface layers

Plasma operations show a complex footprint on the limiter including net erosion and redeposition zones with surface layers (Fig. 1(a)). This global erosion–redeposition pattern is in agreement with only parallel transport of particles along field lines (Fig. 1(b) and (c)). The carbon layers are principally localised in the private flux regions at the boundary between plasma and shadowed area. Some tiles where redeposition is dominant are also located on the wetted area where the magnetic field lines are almost tangential to the surface (close to the LCFS). This tangential zone receives theoretically lower heat and particles loads than the next eroded surfaces (with higher penetration lengths and incident angles) but is of particular interest because of its proximity with the confined plasma.

Because of a low thermal transfer between the deposits and the bulk, temperatures measured on surface layers are much higher

* Corresponding author.
E-mail addresses: sophie.carpentier@cea.fr, sophiecarpentier_1@yahoo.fr (S. Carpentier).

0022-3115/$ - see front matter © 2009 Elsevier B.V. All rights reserved.
doi:10.1016/j.jnucmat.2009.01.246

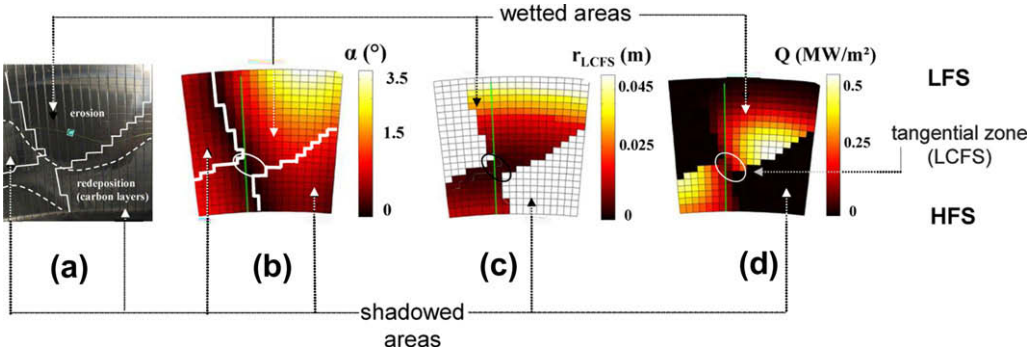

Fig. 1. View of the 20° limiter section supervised by the IR system. (a) Visible image of the limiter showing erosion and redeposition areas. (b) Incident angle of the connected field lines (α, °). (c) Maximum distance to the LCFS (r_{LCFS}, m). (d) Heat flux simulation on the limiter deduced from α and r_{LCFS} maps ($Q_{\text{lim iter}}(r_{LCFS}) = Q_{LCFS}.e^{-\frac{r_{LCFS}}{\lambda_q}}.\sin(\alpha)$ with λ_q = 1.2 cm and Q_{LCFS} = 24 MW/m^2). Solid lines: boundary between shadowed and wetted areas. Dashed lines: redeposition area with carbon layers. White circle: tangential zone (α = 0), defines the separation between the LFS and HFS wetted areas.

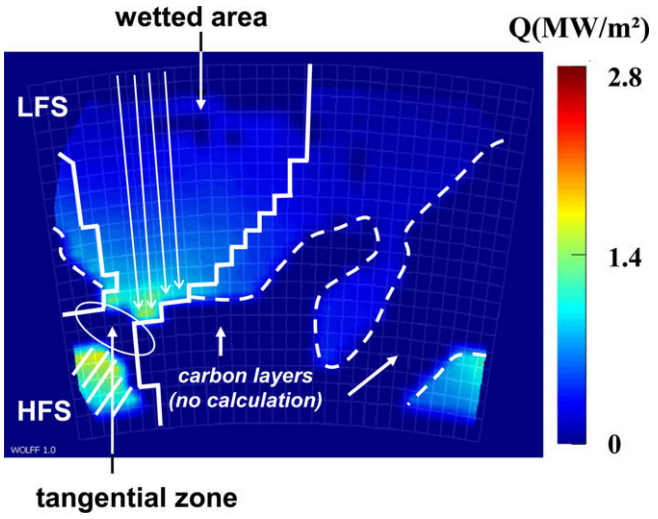

Fig. 2. Experimental heat flux pattern on the limiter. Discharge: 39862 (t = 20 s). Solid lines: wetted areas. Dashed lines: redeposition area excluded from the calculation (with carbon surface layers). Shaded area: heat flux calculation disturbed by thin carbon layers. White lines: profiles drawn to rebuild the Q^{IR}_{SOL} profile (Fig. 3(a)). The maximum heat loads reached 1.5 MW/m^2 on the LFS (not disturbed by thin carbon layers). The lower heat fluxes are contained between 100 and 300 kW/m^2.

than the real surface temperature of the underneath CFC, even for low incident heat fluxes. This overheating prevents from associating directly the whole temperature map to the real heat flux pattern on the limiter. Assuming that carbon deposits actually receive a trifling part of heat fluxes from the plasma, they will be excluded from our thermal calculation.

Sorting tiles and ignoring the redeposition areas is possible using a warping procedure which automatically segment the IR images according to the real geometry of the component. The carbon deposits are then differentiated from clean CFC surfaces (erosion zone) using their typical thermal responses resulting in sharp heating during fast events. The carbon layers pattern shown in Fig. 2 was localized by ignoring tiles presenting a temperature increase higher than 50 °C during a disruption.

2.2. Deconvolution of IR temperatures and coherence with calorimetry

Heat fluxes on the limiter ($Q^{IR}_{\text{lim iter}}$, MW/m^2) are estimated from the 1D linear deconvolution of the temperatures maps ($T^{IR}_{\text{lim iter}}$, °C), using the analytical thermal quadrupole method to model the impulse thermal response of the limiter, as described in [2]. In order to get rid of carbon redeposition between the tiles gap (which occurs everywhere even in erosion zones), the average IR temperatures are given by the values of only few pixels in the centre of each tile. A 2D interpolation of the discrete flux values obtained leads to the experimental heat flux pattern shown in Fig. 2.

The thermal pattern calculated is overall coherent with the erosion–redeposition footprint, with most of heat loads deposited on erosion areas. Nevertheless, on these wetted regions, the heat flux peak is paradoxically localised on a restricted area close to the tangential zone where field lines are low-angled. A more restrictive study has shown that heat fluxes estimated on 10 tiles (see Fig. 2) can be considered as disturbed by the presence of very thin deposits and must be finally ignored. On the other hand, the whole heat flux calculation on other regions is confirmed as not distorted by carbon surface layers.

The heat fluxes estimated from IR data can be compared to the extracted power measured by calorimetry [3]. The toroidal integration of the previous heat flux pattern corresponds to a total incident power of 1.25 MW whereas calorimetry measurements predict 1.15 MW extracted from the cooling component during the stationary phase. In addition, if one suppose that the whole redeposition area receives a uniform incident heat fluxes of 100 kW/m^2 (with ~30 kW/m^2 directly radiated), the total transmitted power into the limiter then increases by 0.2 MW. This additional power is no longer in agreement with the calorimetry balance then 25% overvaluated (versus 8% on the erosion areas only) and indicates that heat fluxes estimated from IR images could also be slightly overestimated. Nevertheless, considering the two diagnostics accuracy, this agreement is satisfactory and confirms that heat fluxes on carbon layers will be marginal in term of power balance.

3. Estimation of the parallel heat fluxes in the SOL

3.1. Estimation using IR data

The heat flux profile in the SOL (Q^{IR}_{SOL}, MW/m^2) can be deduced from the experimental heat loads estimated onto the wetted areas of the limiter considering only parallel heat transport along field lines: $Q^{IR}_{SOL}(r_{LCFS}) = Q^{IR}_{\text{incident}}/\sin(\alpha)$, where α is the incident angle and r_{LCFS} is the radial distance to the LCFS associated to each field lines connected to the limiter (Fig. 1(b) and (c)). The total incident flux on the limiter (Q^{IR}_{incident}) then corresponds to the addition of the heat conducted into the materials (provided by the deconvolution of IR images) with the radiated flux emitted by the surface ($\sigma.T^{IR^4}_{\text{lim iter}}$<5 kW/m^2).

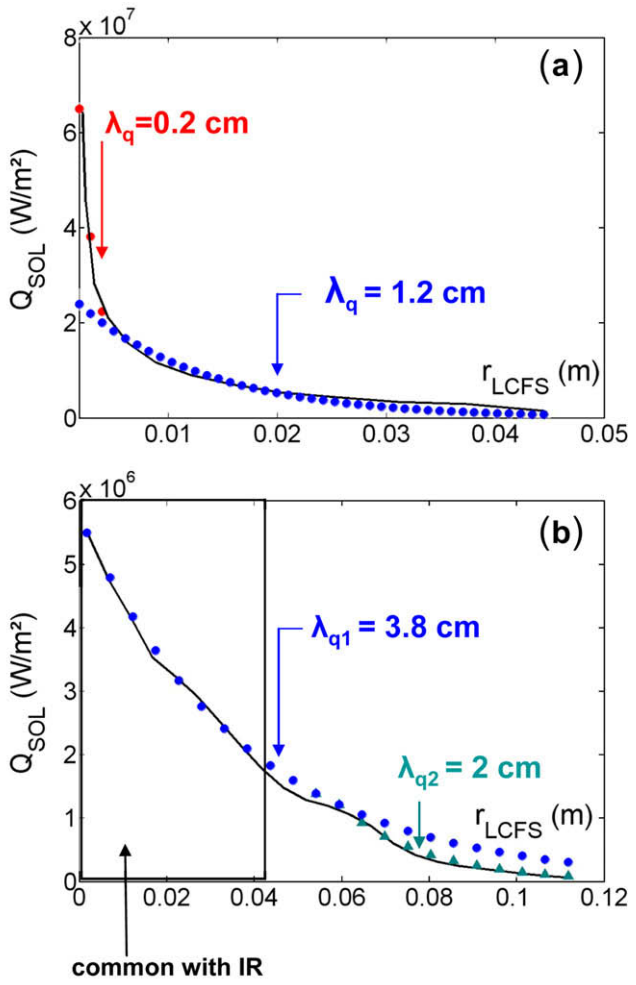

Fig. 3. (a) Average Q^{IR}_{SOL} profile deduced from 4 limiter profiles drawn in the LFS area of the limiter (Fig. 2). Solid circles: exponential decreasing fit with $\lambda_q = 0.2$ cm and $Q_{LCFS} = 65$ MW/m^2 (for $r_{LCFS} < 0.004$ m). Solid triangles: second part of the profile (r> 0,004 m) fitted with $\lambda_q = 1.2$ cm and $Q_{LCFS} = 24$ MW/m^2. (b) Q^{RFA}_{SOL} profile (transmission coefficient $\gamma = 13$ with $T_i = 3.5\ T_e$) showing also two different heat *e*-folding lengths. Solid circles: exponential decreasing function with $\lambda_q = 3.8$ cm and $Q_{LCFS} = 5.5$ MW/m^2. Solid triangles: exponential decreasing function with $\lambda_q = 2$ cm (for $r > 0.06$ m).

The heat flux profile in the SOL is commonly approached by an exponential decreasing function: $Q_{SOL} = Q_{LCFS}.e^{\frac{r_{LCFS}}{\lambda_q}}$ where λ_q represents the heat flux *e*-folding length. The experimental profile calculated from the limiter (Fig. 3(a)) presents two different *e*-folding lengths. The paradoxical presence of high heat loads on the component at the boundary of the tangential zone where incident angles are very low ($\alpha < 1°$) leads to very high heat fluxes and to a stiff profile ($\lambda_q \sim 2$ mm) in the SOL within the first 4 mm from the LCFS. This non standard profile confirms the contribution of complex phenomenon near the tangential zone, added to parallel transport (discussed latter, Section 3.3). Because of the high sensibility of Q^{IR}_{SOL} calculation for low incident angles, this additional contribution can not be clearly quantified and must be ignored if one wants to estimate mainly the parallel transport contribution in the SOL. The whole Q^{IR}_{SOL} profile will be then approached by one exponential function with a λ_q estimated to 1.2 cm and $Q_{LCFS} = 24$ MW/m^2, corresponding to the smooth second part of the profile (where $r_{LFCS} > 0.004$ m and $\alpha > 1°$). This last estimation of λ_q is consistent with former values reported for Tore Supra [6].

3.2. Power balance in the SOL: comparison of IR and RFA probe measurements

Independently of IR measurements, the heat flux density profile was calculated from the data measured by a retarding field analyzer (RFA) [4]. On Tore Supra the RFA is installed on the fast reciprocating drive located in a top port at poloidal angle $\theta = 79°$ with respect to the outer midplane. The probe measures simultaneously the electron temperature (T_e) and the ion one (T_i), as well as the ion saturation current density j_{sat}, parallel to the magnetic field. The fluxes arriving both from low-field side *LFS* and from high-field side *HFS* are measured (Mach probe arrangement). The heat flux densities collected on each side of the probe are calculated as $Q^{RFA\ HFS,\ LFS}_{SOL} = \gamma T_e j^{HFS,\ LFS}_{sat}$, where $\gamma(T_i, T_e)$ is the total heat transmission factor [5]. At the LCFS, Q^{RFA}_{SOL} (Fig. 3(b)) is about a factor of 4 lower compared to Q^{IR}_{SOL} (5.5 MW/m^2 versus 24 MW/m^2), but it is characterized by a three times longer *e*-folding length (3.8 cm compared to 1.2 cm).

The power in the SOL can be reconstructed from RFA and IR measurements using the following expression: $P_{SOL} = 2(2\pi R)\int_{LCFS}^{\infty} dr \frac{B_R}{|\mathbf{B}|} Q_{SOL}$, where R is the tokamak major radius, B_R is the local component of the magnetic field aligned with R, and $\mathbf{B}$ is the local magnetic field vector. It is assumed that the sum of the HFS and LFS power fluxes is the same as the power flux that would be incident on either the ion side or the electron one. Hence, in order to add both strike zones together, the integral is multiplied by a factor of 2 (assuming equal power deposition on each zone). For the DITS scenario $P^{RFA}_{SOL} \cong 0.3$ MW which represents about 25% of $P_{SOL} \cong 1.3$ MW deduced from the total injected power reduced by the radiated power and electron ripple losses. $P^{IR}_{SOL} \cong 0.4$ MW (33% of P_{SOL}) whereas heat fluxes at the erosion area of the limiter are supposed to be lightly overestimated (as shown by the comparison with calorimetry) and could integrate a slight contribution of perpendicular transport, even far from the LCFS. This disagreement with P_{SOL} (given by the power balance) in one hand and between the Q^{RFA}_{SOL} and Q^{IR}_{SOL} profiles on another hand is not yet understood.

3.3. Discussion: comparison with a simple SOL model

In this section, we reason in the reverse direction and start from a theoretical heat flux profile in the SOL to project it onto the limiter. Heat deposition due to the parallel heat transport can be predicted using the 3D magnetic configuration combined with a simple SOL model where the heat flux *e*-folding length λ_q is fixed. This standard heat flux pattern does not correspond to the experimental heat footprint. The theoretical heat flux peak (Fig. 1(d)) is located further away from the tangential zone than the experimental one (Fig. 2) paradoxically localised close to carbon surface layers on the area where incident angles are low.

Previous studies [6] have shown that a few percents of perpendicular heat contribution added to the parallel heat transport in the SOL allow improving the matching between the experimental and the theoretical peak heat flux. The disagreement between the standard pattern and the experimental one can be also explained by the addition of heat fluxes spreading around the initial strike position of each field lines on the limiter [7]. Further investigations are required to state the influence of each one of these contributions and to explain this presence of significant heat loads at the tangential zone, not coherent with the growth of carbon surface layers observed on this area.

4. Conclusion and prospects

Heat flux calculation has been performed on the erosion zone of the toroidal pumped limiter of Tore Supra. It shows quite good

agreement with the extracted power measured by calorimetry. Using the heat fluxes computed on the limiter, we have deduced the heat flux profile in the SOL attributed to the parallel transport contribution. The power balance then obtained remains unsatisfactory regarding to the expected power leaving the confined plasma. On the other hand, it is coherent with the RFA probe measurements whereas a discrepancy is observed between the two diagnostics for both λ_q and Q_{LCFS} estimation.

The major part of the heat flux pattern onto the limiter is in agreement with the particle flux due to parallel transport, and then useful to deduce information in the SOL. Nevertheless, some local phenomenon close to the tangential area, where a peculiar activity has been observed (flaking [1], hot spots [8]) remains not fully understood. Further investigations are required to complete the experimental map on this tangential area and evaluate accurately the heat fluxes deposited on carbon surface layers. The respective contributions of complex mechanisms (perpendicular heat flux, spreading, funnelling effect) probably leading to high heat fluxes close to the LCFS (about five times higher than the theoretical peak heat load calculated on this region) have also to be investigated.

References

[1] B. Pégourié et al., J. Nucl. Mater., 390–391 (2009) 550.
[2] J.-L.Gardarein et al., Int. J. Therm. Sci. 48 (2009), in press.
[3] J.-C. Vallet et al., J. Nucl. Mater. 313–316 (2003) 706.
[4] M. Kočan et al., Rev. Sci. Instrum. 79 (2008) 073502.
[5] P. Stangeby, Inst. Phys. Publ. 646–655 (2000).
[6] R. Mitteau et al., J. Nucl. Mater. 313–316 (2003) 229.
[7] X. Bonnin et al., J. Nucl. Mater. 337–339 (2005) 395.
[8] A.Ekedahl et al., J. Nucl. Mater., 390–391 (2009) 806.